DEVELOPMENT OF A THERMAL MODEL FOR THERMAL MASS COUPLED WITH HYBRID VENTILATION IN AN INSTITUTIONAL BUILDING

Sophie Yuan[1], Andreas Athienitis[1], Yuxiang Chen[2], Jiwu Rao[1]
[1]Building, Civil and Environmental Engineering, Concordia University, Montreal, Canada
[2]Civil and Environmental Engineering, University of Alberta, Edmonton, Canada

ABSTRACT

Coupling thermal mass and hybrid ventilation in buildings can, through night free cooling, reduce the energy consumption and peak electricity demand for space cooling. This study focuses on Concordia University's thermally massive 17 storey high "EV building". Operating in hybrid ventilation, cool outdoor air enters through motorized inlets on opposing façades, flows above 0.4m thick concrete floor towards interconnected atria, and exits at the roof. The addition of variable speed fans installed at the roof assists in pre-cooling the thermal mass and is expected to further decrease the building's cooling energy consumption. This paper presents the development of a thermal model, verified by in situ measurements, of the corridor zone where outdoor air enters the building. It is then used to investigate the rate of heat extraction via night ventilation, the cooling potential, and the allowable lower limit of outdoor air temperature for hybrid ventilation without compromising occupant comfort.

INTRODUCTION

Commercial and institutional buildings' energy consumption in Canada increased from 867 to 1057 PJ from 1990-2010 (Natural Resources Canada, 2013a). Over 50% of it is used for space heating and cooling. Although the portion used for cooling is 5.2% in 2010, its share has grown by 84% from 1990-2010. Space cooling is a great portion of energy use during summer peak hours. In fact, in Ontario, 50% of energy use in commercial buildings is for heating, ventilating and air-conditioning (HVAC) in the 2003 summer peak profile (Hydro One Networks & Hydro One Brampton, 2003).

Commercial and institutional buildings have high occupancy during operating hours and significant plug loads, which can result in requiring cooling even during winter and shoulder seasons. To reduce cooling energy consumption, designers can look at utilizing natural ventilation, or hybrid ventilation instead of solely using mechanical HVAC systems. A building is naturally ventilated when outdoor air is allowed into the buildings through natural forces without any mechanical system involved. There are three types of hybrid ventilation (Santamouris & Wouters, 2006). First is having both natural and mechanical ventilation complement each other. Second is fan-assisted natural ventilation, where fans drive the airflow into the building when there is insufficient pressure difference. Third is stack and wind-supported mechanical ventilation, for mechanical ventilation systems whose pressure losses can be compensated by natural ventilation.

Buildings designed for natural ventilation often make use of known prevalent wind orientation from site assessments for single-sided and cross-ventilation, and thermal buoyancy for stack ventilation (Awbi, 2008). Natural ventilation has many benefits for both the building owner and the occupants. By letting cool outdoor air into the building, not only is the energy consumption for mechanically cooling and recirculating air reduced, but the amount of fresh air is also increased. Occupants in naturally ventilated buildings generally experience fewer occurrences of sick building syndrome compared to those in mechanically ventilated buildings (Seppänen and Fisk, 2002; Muhič & Butala, 2004).

Exposed interior thermal mass in a building amplifies the benefit of free cooling, as it gains heat throughout the day and discharges it over the night. A thermal model can be made to predict the charging and discharging of the thermal mass. The temperature fluctuations of the thermal mass and room can be examined through modeling a room with thermal mass using the harmonic response method, which can be useful in initial design stages (Zhou, Zhang, Lin, & Li, 2008). A full building with many thermal zones can be modeled using data driven thermal model, which is then used for temperature simulations over a few days to weeks, with most zones resulting in root mean square error between 0.3-0.4 °C (Spindler & Norford, 2009). Ultimately, the goal of our project is to have a thermal model be used for model predictive control (MPC) to decide when to use natural ventilation and for how long, in anticipation of forecasted weather conditions.

Concordia University's Engineering, Computer Science, and Visual Arts Integrated Complex (EV building) is a 17 storey and fits in the category of a typical mid- to high-rise commercial and institutional buildings. During its early design phase, analyses were made with regards to the building façade in order to control solar heat gains and daylighting, and lower heating and cooling energy consumption (Tzempelikos, et al., 2007). The resulting design of the building considers fan-assisted hybrid ventilation. EV building has motorized dampers that act as fresh air inlets on its south-eastern and north-western facades, as shown in Figure 1. The building is highly glazed (two thirds of the façade area) and has 5 stacked atria, each with a height of 3 storey, connected by floor grilles that act as a solar chimney to enhance ventilation through stack effect. At the roof, above the atria, there is a 5 m^2 vent with motorized dampers to exhaust air. The inlet and outlet dampers, and floor grilles would open when hybrid ventilation is employed, and supply air from the mechanical system to the main corridors and atria is stopped. The outdoor air is expected to follow the path shown in Figure 2 as it removes heat stored in exposed thermal mass, primarily from the 0.4 m thick concrete floor.

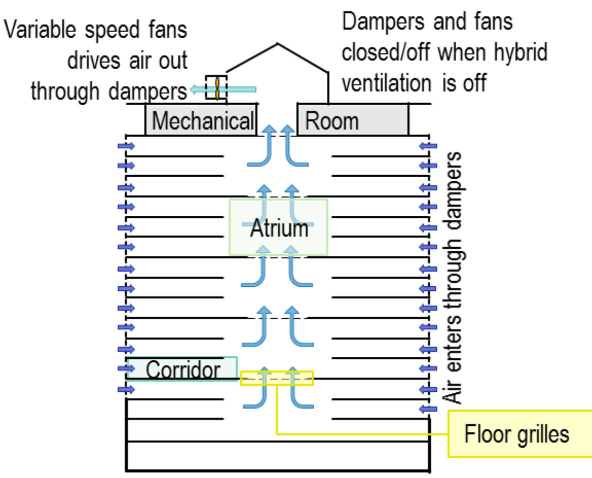

Figure 1: Schematic of EV building's components for fan-assisted hybrid ventilation mode

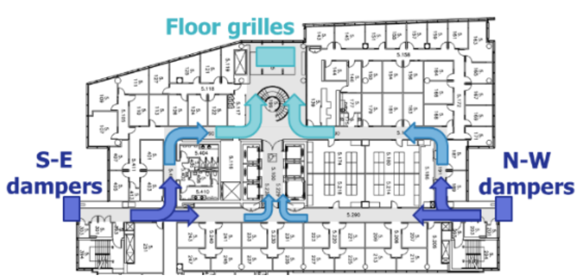

Figure 2: Typical floor plan with expected airflow path of using hybrid ventilation

The addition of 6 variable speed fans at the roof exhaust, near the end of 2015, will be used to enhance the natural ventilation due to stack effect by drawing a total of up to 30,000 L/s air from the outdoors. A weather station, including sensors to measure air temperature and relative humidity, and wind speed and direction is installed on the roof of EV building and records averaged data per minute. Ideally, a relationship can be made in the future to localize forecast data, in order to use it for MPC purposes.

A semi-empirical thermal model, with the concrete floor modeled as a semi-infinite slab, was created for highly massive buildings, using data from the EV building. (Karava, et al., 2012). The study used 3 months' data and estimated that during that time the building's hybrid ventilation system was able to reduce by 30% the cooling requirements for the corridors and atrium. The outdoor temperature range at which air is let into the building is currently between 15-25 °C and its relative humidity below 70 %. For night cooling, it is found that allowing outdoor air at 12 °C to cool 864 m^2 (area of corridors and atria of floors 2-10) of concrete floor will require 6 hours to remove 25 kWh, which is more than the expected cooling energy demand for that zone. The study separated the 30 m long corridor into 10 sections of 3 m length.

The EV building motorized dampers on the façade starts on the second or third floor on the North-West and South-East façade respectively. The 5th floor becomes the first floor with the motorized inlets to also be the bottom floor of an atrium, which would be useful for comparison of data in future data collection of the concrete floor at the atrium. For this reason, the focus of this paper is on the 5th floor, specifically on the corridor in the South-East side. The first 10 m of the corridor is considered, which covers the length from the inlet until nearly the first fork of the corridor. The first few meters from the motorized inlet are generally free of occupants at night, since it is near the emergency staircase, and office spaces are located at the end of the considered portion of the corridor. Narrowing down to the corridor is useful to look at how quickly the air can warm up so that the occasional person present will not feel uncomfortable, in addition to the corridor being the region where the most heat transfer between air and the concrete floor is expected to occur.

METHODOLOGY

This paper presents a simple thermal model of heat removal from thermal mass via night ventilation. The location of interest is the first 10m length of a typical corridor starting from the inlet for outdoor air. Assumptions, such as the corridor's geometry, are made to simplify the model. In addition, data acquired from the EV building is used to simplify and verify the model. Afterwards, by comparing the change in temperature in the concrete's discretized layers along the corridor, the amount of heat removed can be determined.

EXPERIMENT

In order to verify the thermal model, on-site data from the EV building's South-East corridor on the 5th floor was collected. A data acquisition system recorded temperature and air velocity every minute as an average value from samples at 10 s intervals. At 0.4 m height, on the interior side of the dampers, a one directional anemometer measured the velocity of air going perpendicular to the inlet. 25 thermocouples were used; 1 near the anemometer to measure the inlet temperature, and 4 sets of 6 thermocouples placed at 1.5 m, 3 m, 6 m, and 10 m from the inlet, as shown in Figure 3. Each set consists of 3 thermocouples to measure the air temperature at 0.1 m, 1.1 m, and 1.7 m height, 1 thermocouple on each side walls, and 1 thermocouple on the underside of the suspended acoustic tiles. 4 infrared sensors were suspended from the acoustic tiles to measure the floor surface temperature at the same distance from the inlet as the thermocouples.

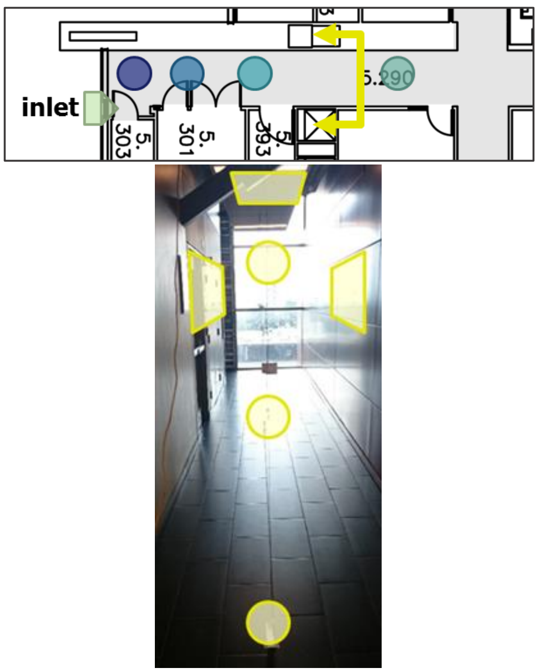

Figure 3: Measurement locations along corridor (top) and cross-sectional view of the corridor (bottom)

In order to be representative of the best case scenario for night ventilation, data collection was performed on the cold night of October 8th, 2015. The forecasted air temperature at the Dorval airport weather station during the hours of operation was between 8-9 °C. The air temperature at the Dorval airport weather station during the day of October 8th reached a high of 12.1 °C late afternoon, dropped to 8.1°C by 2:00 (October 9th), and continues going down to 5.4 °C by 7:00. The weather forecast was close to the measured values for air temperature when night ventilation was used. It is speculated that allowing even colder air into the building may cause discomfort to the occasional occupants working late at night. Data collection having been done late during the shoulder season before winter, the procedure for data collection will be repeated once spring arrives in 2016. However, it is expected to be indicative of the heat transfer processes and the large temperature differential between inside and outside reduces modelling errors.

During the night, night hybrid ventilation was in operation from 22:00 to 2:00, during which the rooftop weather station recorded air temperatures between 7.7-8.9 °C and relative humidity between 54-63 %, whereas the thermocouple placed inside the building at the inlet recorded temperatures between 10.1-14.4 °C. The difference in temperature between the rooftop and the inlet can be due to the air being warmed by the heat released by the building façade, as well as other surrounding buildings, and potentially even the street at low wind conditions. The dampers were closed during the day before 22:00 and immediately after 2:00.

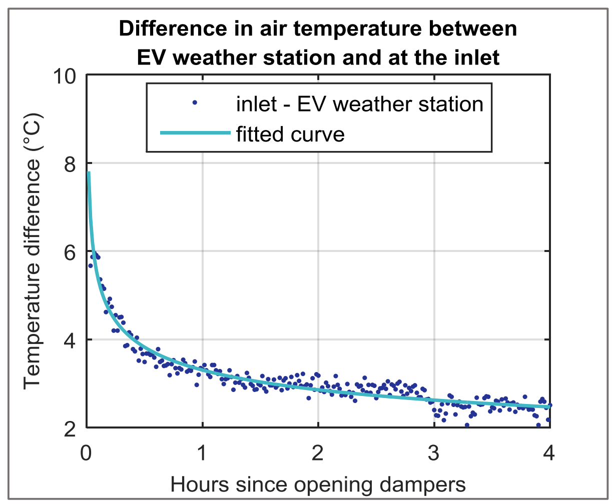

Figure 4: Air temperature difference between the EV rooftop weather station and at the inlet

Natural/hybrid ventilation is often controlled based on the concentration of CO_2 as an indicator of fresh air, outdoor air temperature, or a ratio of indoor and outdoor temperature (Awbi, 2008). For the EV building, it is advantageous to use the exterior air temperature from the rooftop weather station as an input, to reduce the number of sensors needed. To relate the measured air temperature at the inlet to that of the weather station on similar cool nights, their difference with respect to time is approximated as exponential, as shown in Figure 4; thus, the inlet temperature, T_{inlet}, can be calculated, using Equation 1, based on the weather station's measurement, T_{EV}, and time from when hybrid ventilation is turned on, t, in seconds.

$$T_{inlet} = T_{EV} + 16 * t^{-0.2} \quad \text{Eq. 1}$$

The R-squared for this relationship is 0.91, which is close enough to 1, indicating that it describes well the variability in the difference of air temperatures for the given outdoor conditions. On similar cold nights, from Figure 4, it is assumed that there will be at least a 2 ° C difference between the measured air temperature at the weather station and at the inlet. Of course, as the outdoor temperature increases, the temperature difference between the outdoor and indoor environment is expected to decrease, and the Equation 1 would no longer apply.

THERMAL MODEL DEVELOPMENT

An explicit finite difference thermal network model is employed. The model that is developed in this paper simplifies the corridor's geometry and uses calibration factors to account for the geometry, internal heat gains, and radiative heat transfer.

In reality, the corridor has a suspended ceiling consisting of acoustic tiles and lighting elements. Above them are pipes and electrical wires. The model assumes that the corridor ends where the suspended ceiling is and disregards the space above them. Another geometrical simplification is that the bend near the motorized inlets, shown in Figure 3, is neglected. This bend contracts the width of the corridor by 0.35 m, which is small compared to the 1.8 m width of the corridor. The end result of these geometrical assumption results in approximating the corridor as a 1.8 m x 3 m x 10 m rectangular prism. In addition, the thermal model assumes that the inlet for air is the whole exposed façade, instead of a vertical strip near the left.

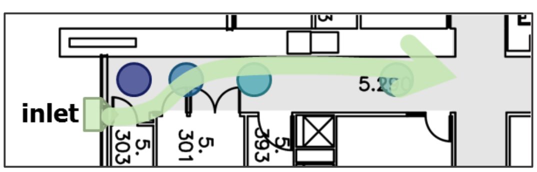

Figure 4: Expected airflow path

Due to that initial bend in the corridor, and the actual inlet being on one side, a recirculation area near the façade and another one along the left wall in the second half of the corridor is expected. Also, the bulk of the incoming air is expected to travel right across the measuring point at 3 m from the façade, as shown in Figure 4, which greatly lowers the average air temperature at that location. In fact, throughout the cool night, the recorded average temperature at 3 m from the façade was consistently slightly colder than at 1 m. In order to account for the expected airflow path, calibration factors are applied to the air velocity between the air nodes in the thermal model.

For practical monitoring of occupied buildings, it is advantageous to use the least amount of visible sensors. The thermocouples placed on the walls and the ceiling are not an option, and its temperatures should be calculated through the model. Therefore, in order to simplify the model, an equivalent temperature for the walls and ceiling is used. It is expected of the air, given the actual geometry of the corridor, to flow towards and interact with the right wall. The ceiling is also expected to be affected due to the buoyancy of air. The combined temperature, henceforth called surfaces temperature, T_{sfc}, is calculated with Equation 2. Using the collected data, a linear regression was performed so that the surface temperature can be calculated using only the inlet temperature and the concrete surface temperature at its control volume as follows:

$$T_{sfc} = \frac{2}{3} * T_{ceiling} + \frac{1}{3} * T_{wall} \quad \text{Eq. 2}$$

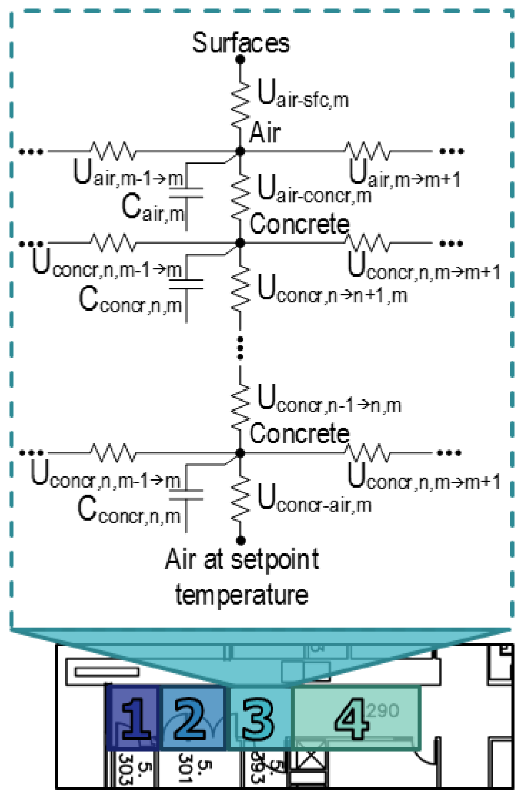

Figure 5: Corridor as 4 numbered control volumes and typical thermal network representation of the 3rd control volume

Figure 5 shows the corridor separated into 4 numbered control volumes, along with a schematic representing the interaction between the outdoor and indoor air, surfaces, and concrete floor. Their associated thermal conductances are denoted as *U*, and thermal capacitances are denoted as *C*.

The thermal conductance between air nodes is defined as in Equation 3, where ρ, c_p, and v are the density, specific heat capacity, and velocity of air. The cross-sectional area of the corridor is represented by *A*.

$$U_{air} = \rho_{air} c_{p_{air}} v_{air}\, A_{corridor} \qquad \text{Eq. 3}$$

Due to the expected flow path mentioned previously, the velocity of air between the different nodes varies. In addition to non-uniformity in the air velocity, backflow due to buoyancy or the recirculation regions is a possibility. As such, the model uses the measured air velocity with a calibration factor for the air velocity between the air nodes along the corridor, such that there is more flow between the first and second air nodes. The calibration factor is 1 between the inlet and the first control volume, 0.6 between the first two control volume, and 0.2 between both the second and third control volume, and between the third and fourth control volume. The summation of the calibration factors along the corridor is equal to 1, indicating that all-in-all the amount of air that enters from the inlet is equal to the amount of air leaving the end of the corridor.

The developed model uses the explicit scheme of finite difference model; therefore, it is important to use a small enough time step that will ensure stability when marching forward in time. The chosen timestep must be lesser than the smallest timestep calculated with Equation 4, where Δt is the critical timestep at node *i*, C_i is the thermal capacity at node *i*, and U_{ij} is the thermal conductance between node *i* and surrounding nodes *j*.

$$\Delta t \leq \frac{C_i}{\sum_j U_{ij}} \qquad \text{Eq. 4}$$

$$\begin{aligned} T_{air}{}_m^{p+1} = T_{air}{}_m^{i} + \frac{\Delta t}{C_{air_1}} \Big[& \rho_{air} c_{p_{air}} v_{air_m}{}^{p} A_{corridor} \left(T_{m-1}^{p} - T_{air}{}_m^{p}\right) + UA_{air-sfc_m} \left(T_{sfc}{}_m^{p} - T_{air}{}_m^{p}\right) \\ & + UA_{air-concr_m} \left(T_{concr}{}_{n,m}^{p} - T_{air}{}_m^{p}\right) + \rho_{air} c_{p_{air}} v_{air_m}{}^{p} A_{corridor} \left(T_{air}{}_{m+1}^{p} - T_{air}{}_m^{p}\right) \Big] \end{aligned} \qquad \text{Eq. 5}$$

$$\begin{aligned} T_{concr}{}_{n,m}^{p+1} = {} & T_{concr}{}_{n,m}^{p} \\ & + \frac{\Delta t}{C_{concr_{n,m}}} \Big[UA_{concr_{n,m-1\to m}} \left(T_{concr}{}_{n,m-1}^{p} - T_{concr}{}_{n,m}^{p}\right) \\ & + UA_{concr_{n,m\to m+1}} \left(Tc_{n,m+1}^{p} - Tc_{n,m}^{p}\right) + UA_{concr_{n\to n+1,m}} \left(T_{concr}{}_{n+1,m}^{p} - T_{concr}{}_{n,m}^{p}\right) \\ & + UA_{air-concr_2} \left(T_{air}{}_m^{p} - T_{concr}{}_{n,m}^{p}\right) \Big] \end{aligned} \qquad \text{Eq. 6}$$

where $A_{air\text{-}concr}$: area of contact between air and concrete (m²)
$A_{air\text{-}sfc}$: area of contact between air and surfaces (walls and ceiling) (m²)
A_{concr}: area of contact between two layers of concrete within and/or in different control volumes (m²)
$A_{corridor}$: cross-sectional area of the corridor (m²)
Δt: timestep (s)
C_{air}, C_{concr}: thermal capacity of air and concrete respectively (J/K)
c_{p_air}: specific heat capacity (J/kg·K)
k: thermal conductivity (W/m·K)
ρ_{air}: air density (kg/m³)
T_{air}, T_{concr}, T_{inlet}, T_{sfc} : temperature of air in the corridor, concrete floor surface, inlet air, and combined surfaces respectively (°C)
T_{concr} : concrete floor surface temperature (°C)
U: thermal conductance or effective heat transfer coefficient (W/m²·K)
v_{air}: air velocity perpendicular to the inlet (m/s)

superscripts *p* and *p+1*: the current timestep number and the following one

subscripts *n*, and *m*: concrete layer number (from top to bottom), and control volume numbers respectively

The energy balance equation at an air node is written as Equation 5, while Equation 6 shows the energy balance at a typical concrete surface node.

The concrete floor is discretized into 10 layers with thin layers near the exposed surfaces, as they experience the most change with respect to time. Symmetrically from the exposed side, the discretized floor's thicknesses is 0.5 cm, 1.5 cm, 3 cm, 5 cm, and 10 cm. The floor's bottom boundary condition is the air from the floor below, which is assumed to be constant at the setpoint temperature of 21 °C. It is usually near 24 °C during summer. Both the air and concrete layers are connected to a capacitance to indicate its thermal capacity, representing its ability to store heat. The air node in this model represents the average air temperature at the three measured heights. In this model, the air is assumed to be well mixed at each control volume.

In order to simplify the model, the heat transfer coefficient between the air nodes and concrete, and between the air and surfaces nodes are assumed to include any effects from the infiltration from door cracks, luminaires, or radiation, which results in higher values than if only convection was considered. Table 1 lists the numbers used in the thermal model. As the airflow affects mostly the concrete floor due to cold air's higher density and gravity, their effective heat transfer coefficient is much higher than those between air and the surfaces. Also, since the air temperature represents the average temperature, and not the temperature near the floor, the coefficients need to be much higher to compensate for the smaller temperature difference between air and the floor surface.

Table 1: Effective heat transfer coefficients between air, surfaces and concrete by control volumes

Effective heat transfer coefficient (W/m²·K)				
Control volume	1	2	3	4
Air – surfaces	4	4	3	2
Air – concrete	9	12	9	8

Table 2: Physical properties of concrete and air

Properties	Concrete	Air
Density, ρ (kg/m³)	1700	1.2
Specific heat capacity, c_p (J/kg·K)	800	1005
Thermal conductivity, k (W/m·K)	1.7	-

In order to be consistent with previous experimental work involving the EV building (Karava, Athienitis, Stathopoulos, & Mouriki, 2012), the physical properties of air and concrete used in this thermal model are identical and shown in Table 2.

The model assumes, as initial values, that the concrete surface temperature is constant throughout its layers in its respective control volume. The air and other surrounding surfaces is assumed to be at the setpoint temperature, since hybrid ventilation was only turned on for the duration of the experiment.

RESULTS & DISCUSSION

Using the measured data for the inlet air temperature and speed, the temperatures of air in the corridor, concrete, and surfaces, were determined. In general, the model is better at simulating the temperature of the concrete surface than air. This is partly due to the assumption of the corridor's geometry.

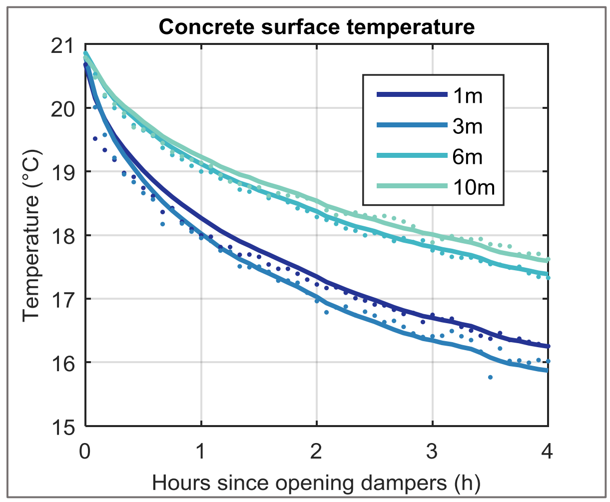

Figure 7: Concrete surface temperature, simulated ones in solid line and experimental ones in dotted lines

The simulated temperatures of concrete, shown in Figure 7, shows that there is two main zones. The first half closer to the inlet will be called primary zone, since it is the region where most of the mixing of the outdoor and indoor air is likely to occur. The latter half will be called secondary zone. The temperature decrease in the primary and secondary zones are 5 °C and 3.5 °C respectively, which is a considerable amount.

On the other hand, Figure 8 shows the simulated and experimental data regarding the average air temperature and the inlet air temperature. The separation of air temperature into two zones can also be seen from the recorded data. There is a drop, within the first half hour of hybrid ventilation, of about 9 and 7 °C in the primary and secondary zones respectively. After the initial drop, the air at the end of the corridor is roughly 3 °C higher than at the inlet. This difference can be expected to be less when outdoor temperatures are higher, since there will be less driving force for the air to enter the building. This is important for foreseeing possible occupant thermal discomfort.

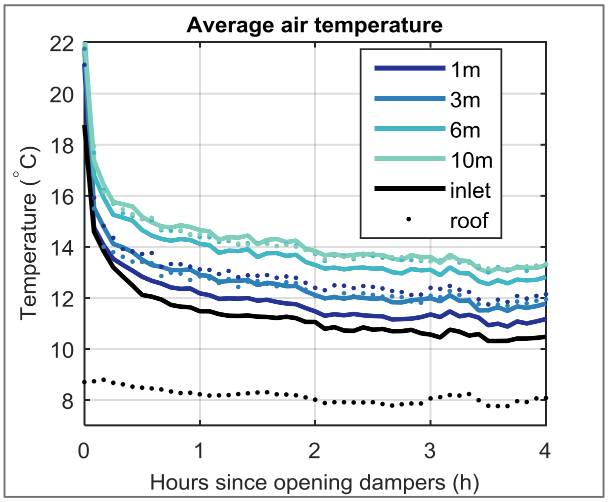

Figure 8: Air temperature, simulated ones in solid line and experimental ones in dotted lines

Throughout the night, the recorded air temperature difference between the measurement at the rooftop weather station and at the inlet drops exponentially from 10 °C to 2.5 °C, indicating that on similar cold nights, this difference can be expected to be at least 2 °C. As the outdoor temperature increases, the temperature difference between the outdoor and indoor environment is expected to decrease. This results in an expected difference of 5 °C between the air temperature at the weather station on the roof and the air at the end of the corridor after a few hours of night ventilation with similar outdoor conditions.

For the EV building, aside from occupants walking through to use the emergency staircase, the corridor is expected to be unoccupied, especially since the closest occupied space is a meeting room located at the end of the corridor. As a result, only the air temperature at the end portion of the corridor is of interest. An acceptable lower limit of air temperature for a month with average temperature of 10 °C and 20 °C are 17.5 °C and 21 °C respectively (ASHRAE, 2004). For the former case, the inlet temperature would need to be at least 14.5 °C; however, as this study is on night ventilation, it is advantageous to extend the boundaries for thermal comfort during unoccupied hours.

If the conditions of that cool night are deemed acceptable, then the minimum inlet air temperature is 10 °C and an increase in free cooling is achieved. Given the expected temperature difference, on cool nights, of at least 2 °C between the temperature at the rooftop and at the inlet, and 3 °C from the inlet to the end of the corridor, hybrid ventilation can be in effect when the temperature measured at the rooftop weather station is between 8 °C and 22 °C. The air temperature during data collection is around the value for the lower limit. The measured data for air temperature, after closing the motorized inlets and stopping hybrid ventilation, quickly rises to 18 °C within half an hour. This suggests that even with this cold condition, hybrid ventilation only needs to be stopped half an hour before occupants are expected into the building in order to avoid discomfort. On the other hand, the upper limit is set based on the indoor temperature setpoint of 24 °C in summer. Allowing exterior air in at this temperature does not offer significant cooling, but is useful as a replacement for the mechanical system that recirculates air within the building, and offers fresh air into the building.

Table 3: RMSE and standard deviation of the error for simulated air temperature.

Air				
Control volume	1	2	3	4
RMSE (°C)	0.96	0.21	0.43	0.16
Standard Deviation (°C)	0.19	0.21	0.14	0.15

Table 4: RMSE and standard deviation of the error for simulated concrete temperature

Concrete				
Control volume	1	2	3	4
RMSE (°C)	0.20	0.14	0.07	0.10
Standard Deviation (°C)	0.15	0.14	0.05	0.09

Back to the simulated data by the thermal model, Tables 3 and 4 show the root mean square error (RMSE) and the standard deviation of the error between the simulated results compared to those recorded. The simulated concrete temperatures show a good agreement with the experimental data, with its RMSE under 0.2 °C and its error expected to be within 0.4 °C. The discrepancy is acceptable for the model, since it is smaller than the error range of the infrared sensors. Comparing the simulated and experimental average air temperatures, the outcome is better for the farther half of the corridor. An error of around 0.4 °C can be expected in the air temperature. The errors for the primary and secondary zones are slightly above and below the 0.5 °C error associated with thermocouple measurements. When dealing with thermal comfort, it is important to determine the air temperature in order to decide when it is too cold to allow outdoor air into the building. While the RMSE is almost 1 °C near the inlet, it is near 0.2 °C at the end of the corridor, where occupants are most likely to be.

Table 5: Heat removed from concrete

Heat extracted from the concrete surface layer to the air				
Control volume	1	2	3	4
4 hours (MJ)	1.991	4.409	3.018	2.308
Total (MJ)	11.726			

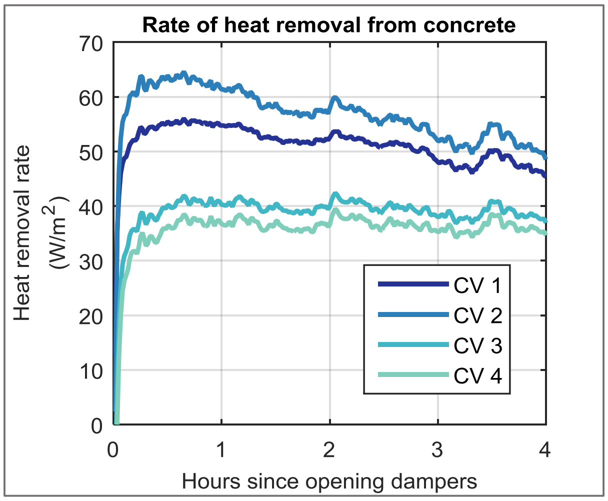

Figure 9: Rate of heat removal from concrete at each control volume (CV) along the corridor

The amount of heat extraction via night ventilation over the 4 hours is shown in Table 5 and the rate of heat removal from the concrete with time is shown in Figure 9. Of course, the location with the most heat removed is in the primary zone, and especially in control volume 2 where the airflow is expected to be passing through. After 4 hours, a total of 11.7 MJ or 651 kJ/m^2 of free cooling is achieved from the concrete floor in the 10 m corridor. From Figure 9, the rate of heat extraction is shown to reach a peak high within the first hour of hybrid ventilation. It appears that the rate of heat removed from the floor is reaching a constant value of 38 and 35 W/m^2 in the secondary zone. On the other hand, in the primary zone, this removal rate is slowly declining by 5 W/m^2·h and would reach a plateau, like the secondary zone, given more time.

After 4 hours of hybrid ventilation, the concrete is cooled down and Figure 10 shows the simulated concrete temperature at different depth along the corridor. Once again, there is a significant temperature difference between the primary and secondary zone, where the primary zone is cooled faster. The initial concrete temperature was linearly interpolated between the measured surface temperature and the setpoint temperature. The figure suggests that for that duration, the effective thermal mass is up to about 25 cm depth, which is slightly more than half of the total concrete floor thickness of 40 cm. This indicates that there is more cooling that can be achieved if hybrid ventilation was allowed to continue for a significantly longer period than 4 hours, even though the rate of heat removal will gradually decrease as mentioned previously.

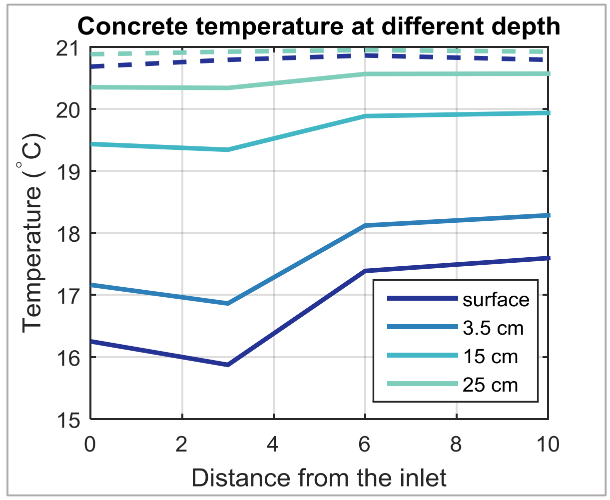

Figure 10: Simulated concrete temperature at different depths, at the start in dashed line, and after 4 hours of hybrid ventilation in solid line

Hybrid ventilation at night is mostly useful during shoulder seasons, and on cool nights in summer, from April to November. Assuming that night hybrid ventilation is on between 21:00 and 6:00, when outdoor air temperature is between the aforementioned 8-22 °C and relative humidity is below 70 %, and using a past weather data of Montreal, there are 94 nights where hybrid ventilation can be employed, for a total of 389 hours, and an average of 4.1 hours per night. A more strict acceptable temperature range of 12-22 °C yields only 75 nights, for a total of 295 hours, meaning 94 hours less of free cooling in a year.

Using the hourly forecasted weather for the Dorval airport instead of the rooftop weather station's measurements, the simulation is run and the resulting RMSE and standard deviation of the error between simulated and measured values for average air and concrete surface temperature is shown in Tables 6 and 7. Generally, the errors are similar when using the measured air temperature at the rooftop and when using the forecast temperature. The total amount of heat removed, shown in Table 8, is 11.3 MJ, about 4% less than the total using the measured air temperature at the rooftop weather station. This suggests that the use of forecast air temperature with this simple thermal model is acceptable, and that it may be used for MPC implementation by predicting how much cooling can be achieved, without overcooling the environment such that it causes discomfort to the occupants.

Table 6: RMSE and standard deviation of the error for simulated air temperature.

Air				
Control volume	1	2	3	4
RMSE (°C)	0.67	0.46	0.27	0.39
Standard Deviation (°C)	0.28	0.34	0.24	0.24

Table 7: RMSE and standard deviation of the error for simulated concrete temperature

Concrete				
Control volume	1	2	3	4
RMSE (°C)	0.30	0.21	0.16	0.16
Standard Deviation (°C)	0.14	0.13	0.05	0.09

Table 8: Heat removed from concrete

Heat extracted from the concrete surface layer to the air				
Control volume	1	2	3	4
4 hours (MJ)	1.922	4.260	2.912	2.225
Total (MJ)	11.319			

With the addition of variable speed fans at the top atrium exhaust, fan-assisted hybrid ventilation can be used. Proper control of the dampers' position as well as the fan speed can increase the airflow into the building, without risk of occupant discomfort from drafts. By increasing the air speed through the building, there is more thermal exchange between the air and building materials, meaning additional pre-cooling. This is particularly useful on nights where there is little wind or the outdoor air temperature is not cool enough to drive a substantial amount of air into the building. A short preliminary test with the fans on and dampers fully open showed that, as expected, the fans affect the upper floors of the building, raising the air inlet velocity from 0.17 m/s at 20 % fan capacity, to 2.83 m/s at 80% fan capacity, and 4.64 m/s at 100% capacity. Clearly, the fan need not operate at 80% or above, during occupied hours, as it will create discomfort to the occupants except at the late night hours when there are no people in the corridors. Controlling the fans and dampers is a study that needs to be carried out in order to reach the system's potential at reducing cooling energy demand while still satisfying occupant comfort. The settings from the future controls system is a means of regulating the inlet air velocity. Ideally, an expanded thermal model can reflect this and accurately simulate temperatures and heat extraction from the thermal mass. These results would then be used as feedback to the controls system to decide how long hybrid ventilation, fan-assisted or not, should be employed.

CONCLUSION

Hybrid ventilation in commercial and institutional buildings can contribute to the reduction of energy required for cooling during shoulder and summer seasons. Data was acquired in the Concordia University EV building, which was designed and constructed for hybrid ventilation through buoyancy and wind forces. These served to verify a finite difference thermal model that was developed for a 10 m portion of the corridor where the motorized dampers are located. The model was made to simulate the physical process of a natural airflow extracting heat from a thermal mass. On a cool night, the corridor could be separated into 2 regions: a primary zone, where most of the heat exchange between air and the thermal mass occurs, and secondary zone. This effect is expected for other mid- or high-rise buildings using a similar hybrid ventilation design.

Through the simulated results for 4 hours of night ventilation, a total of 651 kJ/m^2 of heat is removed from the 10 m corridor segment's concrete floor. The rate of heat removal is highest within the first hour of hybrid ventilation operation, and decreases steadily throughout the remaining 3 hours for the primary zone, while it is almost constant for the secondary zone near its peak value. Flexibility in the range of exterior air temperature allowed into the building can increase the hours of hybrid ventilation, leading to more free cooling. It is suggested for night ventilation to accept outdoor air between 8-22 °C with relative humidity below 70 %, which will result in an indoor air temperature of at least 13 °C at the end of the corridor. With this temperature range, it is also recommended to stop natural/hybrid ventilation half an hour before occupants are allowed into the building, in order to avoid discomfort.

Forecast data for air temperature was used in the model instead of the measured data and yielded acceptable results, with only a 3 % difference in total heat removed from the concrete floor. This seems promising for using forecasted weather data in MPC for quick feedback into the building system control system for natural/hybrid ventilation.

More data collection is expected in spring 2016, when the variable speed fans at the roof can be used with hybrid ventilation for future studies on different outdoor conditions and air velocity.

NOMENCLATURE

A	area (m^2)
C	thermal capacity (J/K)

c_p	specific heat capacity (J/kg·K)
Δt	timestep (s)
k	thermal conductivity (W/m·K)
ρ	density (kg/m^3)
T	temperature (°C)
t	time (s)
U	thermal conductance or effective heat transfer (W/m^2·K)
v	velocity (m/s)

Subscripts

air	air
air-concr	air to concrete floor
air-sfc	air to surfaces
concr	concrete floor
EV	EV building's weather station
i	equation node's number
inlet	inlet
j	nodes' number, surrounding node i
m	control volume number
n	concrete layer number
sfc	combined surfaces

Superscript

p	timestep number

ACKNOWLEDGEMENTS

This work was partly supported by the Natural Sciences and Engineering Research Council of Canada (NSERC), Hydro Quebec, Regulvar, Natural Resources Canada, and Concordia facilities management through a NSERC Industrial Research Chair. The experimental work and instrumentation were supported by the ecoENERGY Innovation Initiative from Natural Resources Canada. The rooftop weather station was established with the support of Environment Canada. The support of Concordia's Facilities Management and Daniel Gauthier is also acknowledged.

REFERENCES

ASHRAE (2004), *ANSI/ASHRAE Standard 55-2004: Thermal Environmental Conditions for Human Occupancy*, ASHRAE.

Awbi H.B. (2008), *Ventilation Systems: Design and Performance*, Taylor & Francis.

Hydro One Networks, Hydro One Brampton (2003), *Electricity demand in Ontario*, http://www.ontarioenergyboard.ca/documents/directive_dsm_HydroOne211103.pdf

Karava P., Athienitis A. K., Stathopoulos T., & Mouriki, E. (2012), 'Experimental study of the thermal performance of a large institutional building with mixed-mode cooling and hybrid ventilation', *Building and Environment*, 57: 313-326.

Muhič S. and Butala V. (2004), 'The influence of indoor environment in office buildings on their occupants: expected-unexpected', *Building and Environment*, 39(3): 289-296.

Natural Resources Canada (2013a), *Energy Use Data Handbook, 1990 to 2010*, http://oee.nrcan.gc.ca/publications/statistics/handbook2010/handbook2013.pdf

Natural Resources Canada (2013b), *Survey of Commercial and Institutional Energy Use: Establishments 2009, Summary Report*, http://oee.nrcan.gc.ca/publications/statistics/scieu/2009/pdf/SCIEU2009Establishments.pdf.

Santamouris M. and Wouters P. (2006), *Building Venitlation: The State of the Art*, Earthscan.

Seppänen O. and Fisk W.J. (2002), 'Association of ventilation system type with SBS symptoms in office workers', *Indoor Air*, 12(2): 98-112.

Spindler H.C. and Norford L.K. (2009) 'Naturally ventilated and mixed-mode buildings – Part I: Thermal modeling', *Building and Environment*, 44(4): 736-749.

Tzempelikos A., Athienitis A.K, and Karava P. (2007), 'Simulation of façade and envelope design options for a new institutional building', *Solar Energy*, 81(9): 1088-1103.

Zhou J. Zhang G. Lin Y. and Li Y. (2008), 'Coupling of thermal mass and natural ventilation in buildings', *Energy and Buildings*, 40(6): 979-986.